

Technique for detecting warm-hot intergalactic gas in quasar UV spectra

Luc Binette, Mario Rodríguez-Martínez, Sinhue Haro-Corzo and Isidro Ballinas
Instituto de Astronomía, Universidad Nacional Autónoma de México, Apartado Postal 70-264, 04510 México, DF, Mexico; binette@astroscu.unam.mx.

ABSTRACT

The ionizing spectral energy distribution of quasars exhibits a steepening of the distribution shortward of ~ 1200 Å. The change of the power-law index from approximately -1 (near-UV) to -2 (far-UV) has so far been interpreted as being intrinsic to quasars. We consider the possibility that the steepening may result from a tenuous absorption component that is anticorrelated with large mass overdensities. UV sensitive satellites, whose detectors can extend down to 1000 Å, can set a useful limit to such an absorption component through the search of a flux increase in the window 1050–1190 Å (observer frame) with respect to an extrapolation of the continuum above 1230 Å. Since the recent FUSE or HST-STIS data do not show any obvious discontinuity in this region, this effectively rules out the possibility that intergalactic H I absorption is very important, and it is concluded that most if not all of the steepening is intrinsic to quasars. A smaller flux discontinuity of order 1% cannot, however, be ruled out yet and would still be consistent with the warm-hot intergalactic component if it amounts to 30% of the baryonic mass, as predicted by some models of large scale structure formation, provided its temperature lies around $10^{5.3}$ K.

Subject headings: galaxies: intergalactic medium — large-scale structure of universe — galaxies: active — radiative transfer — ultraviolet: general

1. Introduction

The ionizing spectral energy distribution (hereafter ISED) of nearby active galactic nuclei cannot be observed directly, due to the large Galactic absorption beyond the Lyman limit. Owing to the redshift effect, however, we can get a glimpse of the ISED from the spectra of distant quasars. The pioneering work of Zheng et al. (1997, ZK97), using HST-FOS archived data, identified a noticeable steepening in quasar SEDs near 1200 Å. The power-law index α ($F_\nu \propto \nu^\alpha$) in quasars steepens from -1 for $\lambda > 1200$ Å to $\simeq -2$ at shorter wavelengths¹, down to 350 Å (λ_{rest}). In a more recent study, Telfer et al. 2002 (hereafter TZ02) found similar results with a composite spectrum characterized by a mean near-UV index of -0.7 steepen-

ing to $\simeq -1.7$ in the far-UV. The above authors favor the interpretation that the steepening is intrinsic to quasars and that it is the signature of a comptonized accretion disk.

On the other hand, certain distributions of intergalactic absorption gas can also cause an (apparent) steepening of the SED, starting at 1200 Å (λ_{rest}), as shown in this Paper, that is, located in the same position as the break encountered by TZ02. As long as ISED studies are based on detectors that do not extend beyond 1200 Å ($\lambda_{obs.}$), one cannot readily distinguish between the contribution to the observed steepening from an intervening absorption model and that of a purely intrinsic break in the quasar SED as proposed by ZK97 or TZ02. FUSE or HST-STIS spectra, however, extend much farther into the UV and will be shown here to provide us with a compelling test to discriminate between the two interpretations.

Large scale structure formation models predict

¹Throughout the text, $\lambda_{obs.}$ and λ_{rest} will denote wavelengths in the quasar rest-frame or in the observer-frame, respectively [$\lambda_{rest} = (1 + z_Q)^{-1} \lambda_{obs.}$].

that a substantial fraction of baryons should reside in a warm-hot phase at current epoch, possibly up to 30–40% of Ω_{bar} . (Davé et al. 2001). Depending on its temperature and distribution with redshift, this warm-hot gas may contribute to a reduced fraction of the observed steepening of the ISED. In this Paper, we show that this component may give rise to a slight flux increase (that is, a discontinuity) in the region 1050–1190 Å (λ_{obs}) with respect to longer wavelengths. The calibration of the level of this discontinuous excess flux can be used as a technique to set useful limits for the baryonic mass contribution from the warm-hot intergalactic component.

The objective (and results) of this Paper is threefold:

1. Find the simplest and yet physically meaningful absorption gas distribution which can mimic the observed steepening (§3.1),
2. Devise a technique to falsify the previous proposition that the break is due to absorption, thereby confirming the idea that the steepening is intrinsic to quasars (§3.2),
3. Propose a dependable technique to reveal traces of a warm-hot baryonic component in the local Universe using UV spectra (§3.3).

2. Procedure and calculations

2.1. Generalized Gunn-Peterson effect

The Gunn-Peterson (GP) effect (Gunn & Peterson 1965) sets stringent limits for the presence of neutral diffuse gas at high redshifts. In the simplest form of the GP test, the absorption gas produces a flux decrement between Ly α and Ly β . The decrement is measured against a continuum level, usually taken to be a power-law extrapolated from the region redward of the Ly α emission line. With high resolution spectra, this technique is sensitive to H I columns otherwise too small to produce resolvable Ly α lines. Songaila, Hu, & Cowie (1999) in this manner could set a limit of the GP opacity $\tau_{GP} < 0.1$ at $z = 4.7$. Another manifestation of the GP effect is illustrated by the staircase transmission curve of Møller & Jakobsen (1990), which is the result of unresolved Ly α forest lines in intermediate resolution spectra. This transmission curve is also characterized by a broad

trough (partly due to photoelectric absorption), the Lyman valley, whose minimum occurs at a rest-frame wavelength ~ 650 Å. Before averaging their quasar spectra, ZK97 and TZ02 statistically corrected each quasar spectrum for the presence of such a Lyman valley by calculating the appropriate transmission curve, using the scheme developed by Møller & Jakobsen (1990). Finally, the GP effect can be generalized to include the broadened wings of faint Ly α forest lines as a result of the Hubble flow in underdense regions.

Our contention is that these manifestations of the GP effect are sensitive to certain classes of H I distributions as a function of redshift. Other H I distributions might instead be associated to large scale voids. In that case, the amount of absorption gas would be decreasing towards the background quasar, against which we are trying to detect it. Such opacity behavior might be harder to pinpoint, since it would not necessarily produce a recognizable absorption break at the rest-frame Ly α . Another factor that could hinder the detection of intergalactic absorption is that the absorption component evolves in the opposite direction as the Ly α clouds, becoming in other words progressively more abundant towards lower redshifts. For instance, hierarchical structure formation is expected to generate a hot gas phase, whose mass is predicted to increase with time (e.g. Phillips, Ostriker, & Cen 2001), that is, with a temporal evolution which is opposite to that of the Ly α forest. Any residual absorption it may cause would occur at much shorter wavelengths, in a wavelength domain too far from the Ly α emission line (λ_{rest}) to rely on an extrapolation of the continuum observed redward of this line.

With these considerations in mind, we have explored various H I distributions, whose absorption behavior is not as evident as that expected from the traditional GP effect. The hypothesis being tested is this Paper is whether all or just a small fraction of the far-UV steepening in F_ν is caused by absorption. We will demonstrate in §3 how this hypothesis is observationally falsifiable. Even if most of the SED break turns out to be intrinsic to quasars, the technique can still be used to set a lower limit on the temperature of the warm-hot intergalactic medium (WHIM).

2.2. Derivation of the transmission curve

The technique used to generate a simulated composite spectrum to compare with the observed spectrum of ZK97 is described in Binette et al. (2002). Briefly, we assume a typical spectrograph sensitivity window for FOS of 1300–3000 Å. We then simply redshift this window in locked steps in order to simulate quasars of different redshifts in the range $0.33 \leq z_Q \leq 3.6$ (the same range as ZK97). Before averaging, each redshifted quasar SED is multiplied by the redshift integrated transmission curve T_λ (defined below). We assume the concordance Λ CDM cosmology with $\Omega_\Lambda = 0.7$, $\Omega_M = 0.3$ and $h = 0.67$ with $h = H_0/100$.

To be definite, we adopt a uniform gas distribution (see Binette et al. 2003). Equivalent calculations assuming a clumpy medium were also carried out for comparison. We found that the ill-defined additional parameters required then do not reveal anything fundamental or even interesting. Furthermore, the two formalisms are equivalent for the assumed opacity regime in which the diffuse absorption component lies in the linear part of the curve of growth, that is for H I columns $N_{H^0} \ll 10^{12} \text{ cm}^{-2}$.

The simulated quasar spectra are divided in energy bins, and for each quasar rest-frame wavelength bin j , we calculate the transmitted intensity $I_{\lambda_j}^{tr} = I_{\lambda_j} T_{\lambda_j} = I_{\lambda_j} e^{-\tau(\lambda_j)}$ by integrating the opacity along the line-of-sight to quasar redshift z_Q

$$\tau(\lambda_j) = \sum_{i=0}^{10} \int_0^{z_Q} \sigma_i(\frac{\lambda_j}{1+z}) n_{H^0}(z) \frac{dz}{dz} dz$$

where λ_j is the quasar rest-frame wavelength for bin j and $n_{H^0}(z)$ the intergalactic neutral hydrogen density, which consists of one of the three density distributions discussed below [eqs (1–3)]. The summation is carried out over the following opacity sources: photoionization ($i = 0$) and line absorption from the Lyman series of hydrogen ($1 \leq i \leq 10$). Although our code could include up to 40 levels, we found that considering only the 10 lowest proved to be adequate. We adopted a fiducial velocity dispersion b of 30 km/s and assumed a Gaussian profile for the σ_i of the lines.

2.3. Heuristic H I gas distributions

2.3.1. Three H I distributions to test

In calculating the transmission function of a quasar at redshift z_Q , we will consider three different distributions of absorption gas density, n_{H^0} , with redshift, which we will then compare with the composite SED of either ZK97 or TZ02. The first is given by

$$n_{H^0}(z) = n_{H^0}^0 (1+z)^3 (1+z)^\gamma (z'_Q)^\beta \quad (1)$$

where z is the absorbing gas redshift, z_Q the quasar redshift, z'_Q the quasar redshift as seen from the absorbing gas at z [that is $z'_Q = (1+z_Q)/(1+z) - 1$], and $n_{H^0}^0$ the neutral gas density at zero redshift. γ and β are adjustable parameters. The $(1+z)^3$ factor represents the cosmological expansion of the Universe. The factor $(z'_Q)^\beta$ with $\beta > 0$ implies that the density decreases in the neighborhood of individual quasars.

The second distribution which will be considered is

$$n_{H^0}(z) = n_{H^0}^0 (1+z)^3 \frac{(1+z)^\gamma}{1+(z_P/z'_Q)^\beta} \quad (2)$$

where z_P is the size of the region (near each quasar) within which the density decreases as $(z_P/z'_Q)^\beta$ towards the quasar [note that $\beta > 0$ as in eq. (1)]. It is possible to substitute the denominator above by the expression $1 + (r_P/r'_Q)^\beta$. For each value of z_P discussed below, we have searched for the value of r_P which would give us an equivalent fit of the composite ISED. The parameter r_P represents the zone of influence (or cavity radius) of the quasars in spatial units. Although the density decreases smoothly towards each quasar, in this text we will refer to this zone, where $r'_Q < r_P$ near each quasar, as a ‘cavity’.

The third distribution is given by

$$n_{H^0}(z) = n_{H^0}^0 (1+z)^3 \frac{\exp[-(z/1.6)^{1.4}]}{1+(z_P/z'_Q)^\beta} \quad (3)$$

where the exponential function in the numerator is a parametric fit to the increase of the warm-hot intergalactic medium (WHIM) towards the current epoch as calculated by Davé et al. (2001) (their Model D2). We will again discuss which value of r_P produces a fit equivalent to that provided by our favored z_P values.

2.3.2. Three conditions to satisfy

The above distributions lie in a sequence of increasing plausibility, as discussed below. We emphasize that our exploration included many more functions than the above three, the vast majority of which could not reproduce a smooth steepening of the spectrum near 1100 Å ($\lambda_{obs.}$) (failing condition *a* below). Nevertheless, these three distributions will suffice for the purpose of unequivocally testing the absorption hypothesis.

In our search, the following procedure was adopted: we explored a large set of functions with the following three priorities in mind: *a*) the n_{H^0} distribution must produce an acceptable fit of the the composite ISED without a discontinuity near Ly α , *b*) it must be a physically meaningful function, and *c*) it must be consistent with other information we have about the Universe such as, for instance, the volume density of quasars. We were able to satisfy conditions *a* and *b*, although *c* could not be strictly respected for our favored test case Model C, as discussed below.

3. Model results

3.1. Reproducing the observed steepening

If we adopt the first distribution of H I corresponding to eq. (1) and the parameters listed in Table 1 for Model A, that is, a zero redshift density $n_{H^0}^0 = 4.7 \times 10^{-12} \text{ cm}^{-3}$, $\gamma = -1.5$ and $\beta = 0.8$, we can reproduce the observed smooth steepening of the composite spectrum of ZK97 remarkably well as shown in Fig. 1 by the thick solid line. The intrinsic SED considered in Model A is a single power-law of index -1 (short-long dashed line), which we extend to all wavelengths. This index provides a good fit at the longer wavelengths (1300–2300 Å) of the underlying continuum in the ZK97 composite spectrum.

This first distribution has also the property that the far-UV index, α_{FUV} , defined in the range 350–900 Å (λ_{rest}), increases very little with quasar redshift (Binette et al. 2003). This agrees with the findings of TF02 (c.f. their Fig. 12). However, although the simplest, this distribution is not physically meaningful in the following aspect: the limitless range of the dependence of eq. (1) on z'_Q implies that the local H I density depends on the quasar redshift. To clarify this point: two inde-

pendent quasars, one nearby and the other at redshift 3, but lying along very nearby line-of-sights on the sky, would be characterized by very different local H I densities according to eq. (1). Such behavior is unphysical, because the H I density in the local Universe should not depend at what distance the background quasar is located. We therefore conclude that condition *b* (‘physically meaningful’, see §2.3.2) is not satisfied and that the n_{H^0} distribution of eq. (1) must be rejected. In the text, we will refer to this undesirable property as the “nearby line-of-sight problem”.

A distribution without any dependence on z'_Q would not suffer from this problem. However, in *all* the distributions that succeeded in reproducing the smooth roll-over near 1200 Å, some kind of smooth gas cavity near each quasar had to be taken in, otherwise, a deep and sharp absorption discontinuity² unavoidably appears at 1216 Å (λ_{rest}) in the synthesized composite SED, a feature that is obviously not observed. The thin long-dashed line in Fig. 1, for instance, illustrates the magnitude of this sharp discontinuity present near Ly α when no cavity is considered (here with β set to zero in eq. (1)).

The solution to this problem is to have the dependence on z'_Q limited to a reduced zone of influence near each quasar. This is achieved with the expression in the denominator in eqs (2) and (3), where z_P limits the distance scale within which the density is decreasing (towards the quasar) as a power-law of index β . We therefore have two competing effects present in our subsequent distributions [of eq. (2) or eq. (3)]: one factor describes the H I density as a function of redshift (seen from us) z , which has no other QSO close to the selected line-of-sight, and the other describes the H I density within the neighborhood of QSOs (within a zone of influence $\simeq r_P$). Two different line-of-sights lying at a projected distance on

²In Binette et al. (2002), such a discontinuity at 1216 Å (λ_{rest}) was smoothed out by invoking photoionization by the background quasar (in analogy with the “proximity effect”). However, the metagalactic background radiation (relative to a single quasar) is much too strong for this proposition to be sustained. Eastman, MacAlpine, & Richstone (1983) avoided the discontinuity by invoking absorption cloudlets being progressively accelerated up to 0.8c within a region < 10 kpc near the background quasar. The main problem was that the cloudlets themselves emitted more UV than the background quasar.

the sky greater than r_P will be described by a unique and self-consistent distribution of H I with redshift. As a consistency check, the volume occupied by all the QSO cavities must be smaller than the total volume sampled.

A possible interpretation of the decreasing density towards individual quasars is that our putative H I distribution is associated to the largest scale voids. The environment of quasars might also be hotter and transparent as a result of (protocluster) stellar winds from the associated large scale and most massive structures. Our aim will be to make z_P as small as possible, but without producing any discontinuity or dip near 1200 Å. The short-dashed line in Fig. 1 shows that the distribution corresponding to eq. (2) (Model B) results in as good a fit to the ZK97 spectrum as Model A, when using $\gamma = -3.0$, $z_P = 0.7$ and $\beta = 1.5$ (see Table 1).

Nevertheless, this Model B is not satisfactory. In effect, a cavity with $z_P = 0.7$ requires a cavity of size $r_P \sim 2$ Gpc, which is more than half the path-length to the highest- z quasar in the sample (i.e. 3.75 Gpc for $z_Q = 3.6$). Hence most line-of-sights would cross many overlapping cavities (hence condition b is not satisfied) and such a situation not properly described by eq. (2). Condition c ('consistency with other reliable information', see §2.3.2) is not respected either. First, the cumulative volume of quasar influence on H I exceeds 15% of the total volume sampled. Second, the exponent of $(1+z)$, $\gamma = -3.0$, is much too steep if we were to compare our Model B to model-predictions of the evolution of the WHIM. For instance, most models in Davé et al. (2001) are characterized by redshift-averaged values of γ in the range -1.1 to -1.5 .

In order to ensure a physically more meaningful H I distribution, we replaced the (γ) power-law dependence on redshift by an exponential fit to the WHIM Model D2 of Davé et al. (2001), the description of which lies in the numerator of eq. (3). Replacing the previous best fit distribution with $\gamma = -3$ by a distribution that matches the behavior of the WHIM with redshift better [by using either eq. (3) or $\gamma \simeq -1.2$ and eq. (2)] comes at a price, however. In effect, such distributions always result in a smooth rise in transmission towards the short wavelength extremity of the SED, beyond 500 Å. Interestingly, the more recent composite

spectrum from TZ02 presents such a rise in the far UV as displayed in Fig. 2. TZ02 have questioned the reality of this rise. The latter might be caused by a tendency of high redshift quasars to have a harder ISED. Nonetheless, because the TZ02 work contains more objects than the ZK97, and because this feature is seen in both radio-loud as well as radio-quiet quasars, we will take their results at face values and compare their radio-quiet composite SED with models which used eq. (3). The thick solid line in Fig. 2 represents our Model C, which is characterized by a significantly smaller $z_P = 0.3$. Although the fit is imperfect, it matches the overall trends present in the TZ02 composite spectrum. The adopted intrinsic SED used here is somewhat harder, corresponding to an index of -0.72 (which is the value inferred by TZ02).

For Model C, with $z_P = 0.3$ we find that $r_P = 800$ Mpc. A single cavity occupies therefore 1% of the total volume sampled. Using the known luminosity function of bright QSOs [i.e. a quasar density of order $\xi = 3 \times 10^{-7}$ Mpc⁻³ (Boyle 2001)], the volume³ corresponding to this value of r_P is too large by a factor ~ 650 and condition c is therefore not fulfilled on the ground of the known density of QSOs. With this caveat in mind, we proceed to study the behavior of the absorption of our putative intergalactic component at wavelengths shorter than provided by HST-FOS. This will allow us to calibrate a new method to detect the WHIM and, indirectly, to determine to what extent condition b is satisfied in Model C.

3.2. Prediction of a possible discontinuity in the far UV

3.2.1. Analysis of the transmission curves

The derivation of the composite SED of Model C required using eq. (3) and calculating the transmission function at evenly spaced redshift values. We now turn to the particularities of these transmission curves. Two such transmission curves are presented in Fig. 3 for illustrative purposes for quasars of redshifts 2.76 and 0.33. Clearly, the main opacity source is the Ly α line. The contribution of photoelectric absorption to the total opacity is relatively small as illustrated in the Fig-

³That is, one should realize the condition $V_Q = \frac{4}{3}\pi r_P^3 \lesssim \xi^{-1}$.

ure while the contribution of higher series lines can be appreciated by the reduced size of the jumps that are visible in the transmission curves. The main result to emphasize is that a discontinuity appears to the blue of $\text{Ly}\alpha$ ($\lambda_{\text{obs.}}$) (that is beyond the UV limit of the HST-FOS detector) in all the calculated transmission curves, not only when assuming the parameters of Model C, but in all the HI distributions that satisfied condition *a* (‘good fit’, see §2.3.2).

By comparing the transmission curves in Fig. 3 with those resulting from $\text{Ly}\alpha$ forest absorbers, a clear difference emerges. The transmission functions derived by (Møller & Jakobsen 1990) (or ZK97) are characterized by a stair-case behavior, in which the opacity from each physical process (either a Lyman series line or photoelectric absorption) *decreases* towards shorter wavelengths, due to the strong evolutionary nature of the $\text{Ly}\alpha$ forest, in which the density of absorbers increases steeply with redshift. In the case of the transmission resulting from equations (1)–(3), the opacity (along a given step of the staircase transmission curve) tends to either remain high or increase towards shorter wavelengths (but, of course, only up to the threshold wavelength of the absorption process involved). The obvious reason for this marked difference is that the HI distributions used here are characterized by a density that increases towards smaller redshifts z .

An inspection of Fig. 3 suggests that, rather than looking for a sharp absorption edge near $\text{Ly}\alpha$ in the quasar rest-frame, the most obvious demarcation produced by $n_{\text{H}\text{I}}^0$ distributions (which satisfy condition *a* of a ‘good fit’) is at the shorter wavelength end, in the 1190–1070 Å observer-frame region where $\text{Ly}\beta$ rather than $\text{Ly}\alpha$ dominates the absorption. In order to detect such a discontinuity near 1216 Å ($\lambda_{\text{obs.}}$), one requires detectors with a sensitivity, which extends to wavelengths shorter than the earlier HST-FOS window, such as provided by FUSE or HST-STIS.

3.2.2. Operative measurement of the jump: τ_{1160}

In order to test our absorption hypothesis against individual quasar spectra observed by STIS or FUSE, we must first calibrate the depth of the expected discontinuity (on the blue side of local $\text{Ly}\alpha$) as a function of $n_{\text{H}\text{I}}^0$ for our different models. Since the intrinsic far-UV spectral index,

α_{FUV} , is not precisely known and, as suggested by the substantial scatter found by TZ02, may even vary from quasar to quasar, it makes sense to measure the depth of the jump in a way that does not depend on an a priori knowledge of the intrinsic ISED. The technique proposed here is to evaluate the discontinuity’s depth at 1160 Å ($\lambda_{\text{obs.}}$) by comparing the flux there to the extrapolated value from a power-law fit redward of $\text{Ly}\alpha$ ($\lambda_{\text{obs.}}$), within the narrow window 1260–1360 Å. This window is meant to exclude the Galactic $\text{Ly}\alpha$ absorption trough as well as the geocoronal $\text{Ly}\alpha$. We define the quantity $\tau_{1160} = \log [F_{\text{obs.}}^{1160} / F_{\text{extr.}}^{1160}]$, which can be shown to be insensitive to the power-law index of the intrinsic ISED assumed. In Fig. 3, we illustrate the procedure by taking as example the transmitted SED of a $z_Q = 1.0$ quasar and Model C (the calculation assumes an ideal detector without wavelength coverage limitations). The two squares illustrate the position (albeit here in the quasar rest-frame), at which it is proposed to define τ_{1160} . For each model discussed (A–D), we list in Table 1 the value of τ_{1160} evaluated at $z_Q = 1$, while in Fig. 4 we plot the behavior of τ_{1160} as a function of z_Q .

3.2.3. Condition *b* and the behavior of τ_{1160}

As discussed in §3.1 concerning the “nearby line-of-sight problem”, it is unphysical to have the local density vary when the background quasar, for instance, lies at redshift 2 rather than 3. We can easily find out when a distribution suffers from this problem by checking whether or not τ_{1160} is constant at moderate and high values of quasar redshift. It is apparent in Fig. 4 that Models A and B suffer severely from the above-mentioned problem. In the case of Model C, however, τ_{1160} is flat, at least beyond $z_Q \gtrsim 0.6$. However, within a radius around us given by the large value of $r_P \sim 800$ Mpc, we may reasonably expect to lie within the zone of influence of a (dominant) quasar. In this case, rather than the smoothly increasing function depicted in Fig. 4, a single value of $\tau_{1160}^{\text{obs.}}$ may instead apply (τ_{1160} reflects the local HI density). Its value would depend on our distance from this dominant quasar. Furthermore, τ_{1160} would not necessarily be isotropic. In conclusion, the smooth initial rise of τ_{1160} in Model C is at best an idealization. Given the likelihood of being positioned inside the cavity of a single quasar, the predicted

τ_{1160} constitutes an upper limit (a more probable value may lie a factor of a few lower).

3.2.4. Negative results using two EUV quasar spectra

We now use Model C as a test case, since it is the most physical at hand under the assumption that the 500 Å rise in the composite ISED of TZ02 is real and that the break is entirely due to intergalactic absorption. For any quasar $z_Q > 0.5$, one finds that τ_{1160} is quite significant. Typically, $\tau_{1160} \gtrsim 0.25$ as seen in Fig. 4. If that much absorption were present, it would therefore be a striking feature in the far-UV spectra [provided the quasar could be observed blueward of 1200 Å ($\lambda_{obs.}$)]. It turns out, however, that the observations of the quasar HS1543+5921 by (Bowen, Tripp, & Jenkins 2001, $z_Q = 0.807$) with STIS and HE2347–4342 by (Kriss et al. 2001, $z_Q = 2.885$) with FUSE, show no indication at all of a discontinuity at the expected level of $\tau_{1160} = 0.27$ and 0.28, respectively, in the 1160 Å region, as compared to the extrapolation from the 1270 Å region. We consider that a discontinuity as small as $\tau_{1160} = 0.05$, if present in the two spectra, would have been apparent.

We conclude that intergalactic absorption cannot be the main cause of the observed steepening in the composite SED. Model C fails not only because of the observed absence of a discontinuity in the far-UV but also because it is inconsistent with the known density of quasars (condition *c*). No other H I distribution could be found that would solve all three conditions. Our study therefore confirms that the change of slope near 1100 Å must be in origin intrinsic to quasars, as proposed by ZK97 and TZ02. This general conclusion is not dependent on the particular distribution adopted, since in all the distributions we have explored (which satisfied condition *a*), τ_{1160} was always ≥ 0.2 when $z_Q > 0.5$.

3.3. Detecting the WHIM in absorption

Having recognized that most of the break is intrinsic to quasars, we now turn to the problem of determining how much flux discontinuity near 1160 Å (i.e. τ_{1160}) can be expected if we assume the H II density predicted by WHIM models and a fiducial temperature of $10^{5.3}$ K. For this purpose, we adopt an intrinsic SED, which already incorpo-

rates the intrinsic far-UV steepening. It consists of a broken power-law, which has the same index of -0.72 in the near-UV as in Fig. 2, but that sharply turns over at 1200 Å (λ_{rest}) into a steeper index of -1.57 in the far-UV, as represented by the short-long dashed line in Fig. 5. These two indices correspond to the values characterizing the radio-quiet quasar composite of TZ02 while the turn-over wavelength is within the range of values encountered by TZ02 (≈ 1200 –1300 Å).

3.3.1. Model D using a broken power-law SED

Adopting eq. (3) and the above broken power-law, we first determine which values of $n_{H_0}^0$ and z_P best reproduce the observed composite SED. The result is Model D, plotted as the solid line in Fig. 5. The same $\beta = 1.5$ is used as for Model C and z_P could now be set to the small value of 0.08 without producing any significant discontinuity⁴ on the blue side of the quasar Ly α emission line. Model D succeeds rather well in fitting the TZ02 composite. It does not constitute, however, a unique solution because of the uncertainties regarding the intrinsic SED. If for instance, we shifted the break from 1200 to 1100 Å, the assumed ISED would lie higher above the composite of TZ02 and a higher density WHIM would therefore be required for the model to overlap the data.

With a predicted value of τ_{1160} as small as 0.05 (see Table 1), Model D is characterized by a much smaller discontinuity than Models A–C, simply because the assumed ISED is much closer to the observed composite of TZ02. Furthermore, τ_{1160} does not depend on redshift anymore, as shown in Fig. 4, which indicates that the cavity near the individual quasars is not affecting our determination of $n_{H_0}^0$. Inspection of the published spectra of HS1543+5921 by (Bowen, Tripp, & Jenkins 2001) and HE2347–4342 by (Kriss et al. 2001) suggests, however, that $\tau_{1160}^{obs.}$ is likely to be smaller than 0.05. A thorough analysis aiming at setting stringent upper limits on $\tau_{1160}^{obs.}$ would clarify the matter.

⁴The value of r_P which can provide an equivalent fit is 200 Mpc. Interestingly, this value is only a factor of two too large with respect to the density of quasars at high redshifts. This can be resolved if we use a function r_P of redshift such as $300(1+z)^{-1}$ Mpc. Although r_P is then larger in the local Universe, at redshifts ~ 2 we get $r_P \simeq 100$ Mpc, which is the epoch when the density of quasar is known to peak. Condition *c* is marginally satisfied in Model D.

3.3.2. Deriving τ_{1160} from the expected WHIM

Let us now turn to the inverse problem of determining the height of the jump τ_{1160} expected from a WHIM component that would contribute 30% of the total baryonic mass in the local Universe (as in Model D2 of Davé et al. 2001). One advantage of the operative definition of τ_{1160} proposed in §3.2.2 is that the choice of a given intrinsic SED is not critical to the purpose of determining $n_{H^0}^0$. This is verified from Table 1 where the quotient $n_{H^0}^0/\tau_{1160}$ evaluated at $z_Q = 1$ in Models C and D are 1.89×10^{-11} and $1.80 \times 10^{-11} \text{ cm}^{-3}$, respectively. They differ by only 5%, despite the use of very different intrinsic SEDs. Because $n_{H^0}^0$ scales linearly with τ_{1160} , all the information needed to derive τ_{1160} can be extracted from Model D independently of whether or not the density inferred turns out very different than in Table 1 or whether the ISED assumed is somewhat incorrect.

For any arbitrarily small *observed* discontinuity $\tau_{1160}^{obs.}$, the inferred H I density is given by $n_{H^0}^0 = 1.8 \times 10^{-11} \tau_{1160}^{obs.} \text{ cm}^{-2}$ which does not depend on z_Q because we have $z_P \ll 0.4$. In terms of the critical density $3H_0^2/8\pi Gm_H$, this density becomes

$$\Omega_{WHIM} = \frac{1.6 \times 10^{-6}}{x h^2} \tau_{1160}^{obs.} \quad (4)$$

where x is the neutral fraction of the putative WHIM absorption gas component. We can express Ω_{WHIM} as a fraction F_b of the (current epoch) total baryonic mass $\Omega_{bar.} = 0.021 h^{-2}$

$$F_b = \Omega_{WHIM}/\Omega_{bar.} = \frac{7.6 \times 10^{-5}}{x} \tau_{1160}^{obs.} \quad (5)$$

With $F_b = 0.3$, we obtain that $\tau_{1160}^{obs.} \simeq x/2.5 \times 10^{-4}$. Since the WHIM is likely to be highly ionized, we are lead to expect very small values of $\tau_{1160}^{obs.}$. For example, for a collisionally ionized WHIM at a temperature $10^{5.3} \text{ K}$, we derive $x \sim 3.1 \times 10^{-6}$ and therefore $\tau_{1160}^{obs.} = 0.012$. Clearly, a high S/N spectrum is required in order to be able to detect a 1% excess flux at 1160 \AA . It remains nevertheless a worthwhile exercise to carry out, since any limit that can be put on $\tau_{1160}^{obs.}$ would directly translate into a lower limit on the neutral fraction (hence on the temperature) of the WHIM component. Note that, with that small $\tau_{1160}^{obs.}$, we have the liberty to set z_P to zero in eq. (3) and condition c (§2.3.2) is therefore implicitly satisfied. By the same token, we do not have to worry about whether we possibly lie in the zone

of influence of a single quasar anymore. In order to optimize the detection sensitivity, the strategy to follow would be to add together as many EUV quasar spectra as possible (ideally with redshift in the range $0.5 \lesssim z_Q \lesssim 0.8$) and then extract $\tau_{1160}^{obs.}$ from the summed stack.

4. Conclusions

In all the distributions of $n_{H^0}(z)$ used for reproducing the steepening observed in the energy distribution of quasars, the dominant atomic process contributing to the opacity is Ly α scattering. An important implication of these calculations is that the transmission curve shows a significant discontinuity to the blue of Ly α ($\lambda_{obs.}$) where the transmission rises sharply. The size of the discontinuity, τ_{1160} , for any distribution of intergalactic gas that can successfully reproduce the SED steepening reported by TZ02 (assuming a single power-law SED), is predicted to be typically > 0.25 in spectra of quasar redshift $z_Q > 0.5$. Since the two quasars HS1543+5921 and HE2347-4342, which were observed by HST-STIS and FUSE, respectively, do not show any sign of a discontinuity anywhere near this level, we consider the case proven that most if not all of the 1200 \AA continuum steepening is intrinsic to quasars rather than due to H I absorption. On the other hand, a small flux increase by as little as 1% percent is still possible and would be consistent with a WHIM temperature $\sim 10^{5.3} \text{ K}$ contributing up to 30% of the current baryonic matter.

This work was supported by the Mexican Science Funding Agency CONACyT under grant 32139-E. We are indebted to Wei Zheng and Randal Telfer for sharing their published composite spectrum which are used in Fig. 1 and 2, respectively. We are grateful to V. Avila-Reese for constructive discussions about the manuscript.

REFERENCES

Binette, L., Rodríguez-Martínez, M., & Ballinas, I. 2002, in ASP Conf. Series, Galaxies: the third dimension, ed. Rosado, M., Binette, L. & Arias, L. (San Francisco: ASP), 282, 317

Binette, L., Rodríguez-Martínez, M., & Ballinas, I. 2003, in Revista Mexicana de Astronomía

y Astrofísica, Conf. Series, Galaxy Evolution: Theory and Observations, ed. V. Avila-Reese, C. Firmani, C. Frenk & C. Allen (Mexico City: Mexico), in press (astro-ph/0205139)

Boyle, B. J. 2001, Advanced Lectures on the Starburst-AGN, Edited by Itziar Aretxaga, Daniel Kunth, and Raúl Mújica. Singapore: World Scientific, p. 325

Bowen,D.V., Tripp, T. M., & Jenkins, E. B. 2001, AJ, 121, 1456

Davé, R., et al. 2001, ApJ, 552, 473

Eastman, R. G., MacAlpine, G. M., & Richstone, D. O. 1983, ApJ, 275, 53

Gunn, J.E., & Peterson, B. A. 1965, ApJ, 142, 1633

Kriss, G. A., et al. 2001, Science, 293, 1112

Møller, P., & Jakobsen, P. 1990, A&A, 228, 299

Phillips, A. A., Ostriker, J. P., & Cen, R. 2001, ApJ, 554, L9

Songaila, A., Hu, E. M., & Cowie, L. L. 1999, ApJ525, L5

Telfer, R. C., Zheng, W., Kriss, G. A., & Davidsen, A. F. 2002, ApJ, 565, 773 (TZ02)

Zheng, W., Kriss, G. A., Telfer, R. C., Grimes, J. P., & Davidsen, A. F. 1997, ApJ, 475, 469 (ZK97)

TABLE 1
MODEL PARAMETERS

Label	Equation (#)	SED $\lambda < 1200 \text{ \AA}$	$n_{H0}^0(z = 0)$ (cm^{-3})	γ	β	z_P	τ_{1160} ($z_Q = 1$)
A	(1)	ν^{-1}	4.7×10^{-12}	-1.5	0.8	—	0.306
B	(2)	ν^{-1}	1.5×10^{-11}	-3.0	1.5	0.70	0.628
C	(3)	$\nu^{-0.72}$	5.2×10^{-12}	—	1.5	0.30	0.275
D	(3)	$\nu^{-1.57}$	9.0×10^{-13}	—	1.5	0.08	0.050

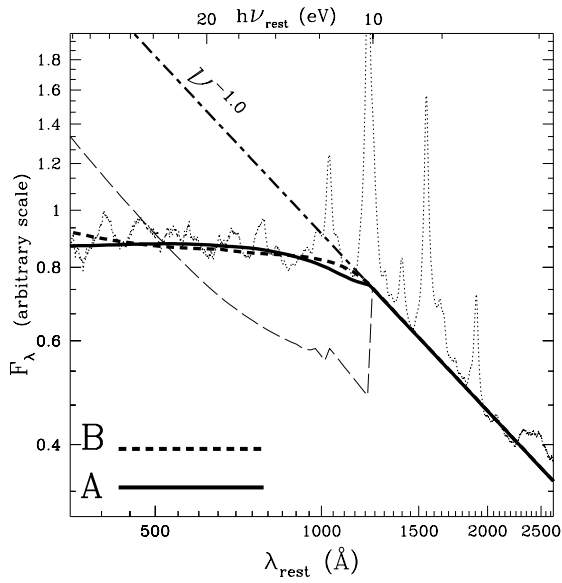


Fig. 1.— The dotted-line in this F_λ vs λ_{rest} plot represents the composite quasar spectrum of ZK97. The straight short-long dashed line represents a power-law fit, in the longer wavelength region $\lambda > 1200 \text{ \AA}$ (λ_{rest}), of the continuum underlying the emission lines. The thick solid line overlaying the ZK97 data is our simulated composite Model A, which assumes a single power-law with $F_\nu \propto \nu^{-1}$ to describe the intrinsic quasar SED and a tenuous H I absorption screen defined by eq. (1) with the parameters listed in Table 1. The short-dash line represents Model B, in which the H I distribution corresponds to eq. (2) with $z_P = 0.7$. The thin long-dashed line illustrates how deep the discontinuity at $\lambda_{obs.} = 1216 \text{ \AA}$ is in models without z'_Q dependence (i.e. without cavity, the curve shown was obtained by setting $\beta = 0$ in Model A).

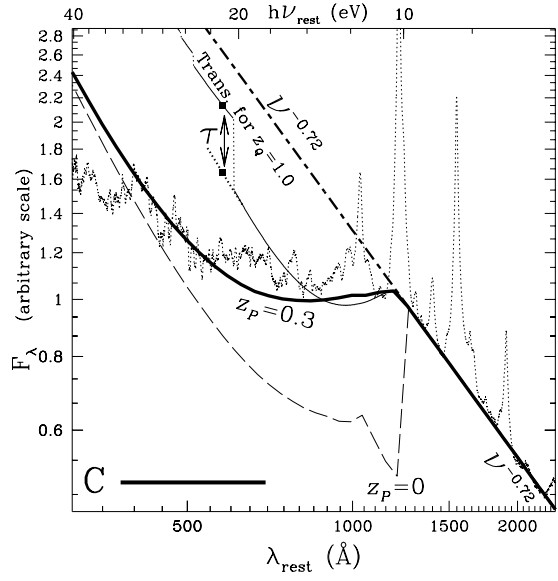


Fig. 2.— The dotted-line in this F_λ vs λ_{rest} plot represents the composite spectrum of radio-quiet quasars by TZ02. The straight short-long dashed line represents a power-law fit (of index -0.72), in the longer wavelength region $\lambda > 1200 \text{ \AA}$ (λ_{rest}) of the continuum underlying the emission lines. The thick solid line overlaying the TZ02 data is our composite Model C, assuming a single power-law, $F_\nu \propto \nu^{-0.72}$, for the intrinsic quasar SED, and a tenuous H I absorption screen described by eq. (3) with the parameters listed in Table 1 ($z_P = 0.3$). The staircase thin continuous line represents the transmitted spectrum for an *individual* quasar of redshift $z_Q = 1.0$, assuming eq. (3) [Model C] and an ideal detector with sensitivity at all wavelengths. The natural logarithm of the flux jump between the two filled squares is τ_{1160} (see definition in § 3.2.2). The thin long-dashed line illustrates the discontinuity at $\lambda_{rest} = 1216 \text{ \AA}$ if we set z_P to zero in Model C (i.e. without cavity).

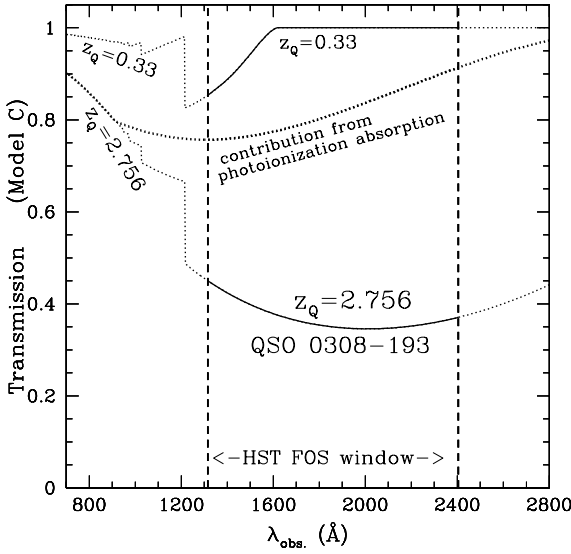


Fig. 3.— The lower solid line is the calculated transmission curve for the quasar 0308–193 at $z_Q = 2.756$ as a function of the *observer-frame* wavelength for Model C [see eq. (3) and Table 1]. The dotted lines shows the continuation of the transmission curve outside the HST-FOS spectral window used on that occasion (1315–2400 Å). Starting from the right, the first, second and third ramps, seen in the transmission curve, are dominated by the opacity of Ly α , Ly β and Ly γ lines, respectively. The line labeled “contribution...” illustrates the small contribution of photoionization to the total opacity. The upper solid line is the transmission curve for a lower redshift quasar at $z_Q = 0.33$.

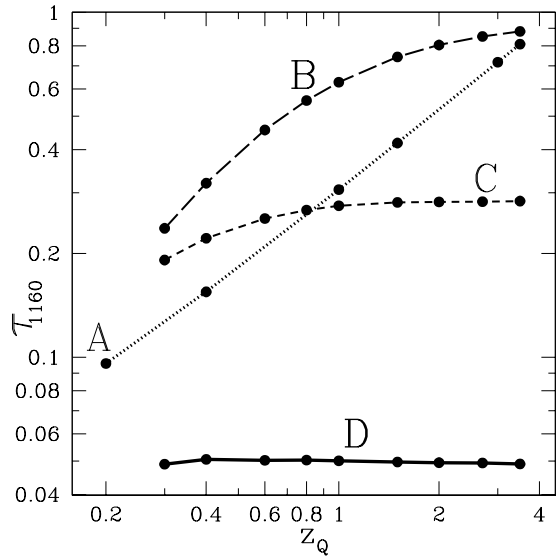


Fig. 4.— Behavior of the depth of the flux discontinuity, τ_{1160} , evaluated at 1160 Å ($\lambda_{obs.}$) (c.f. § 3.2.2), as a function of quasar redshift z_Q for the Models A, B, C and D.

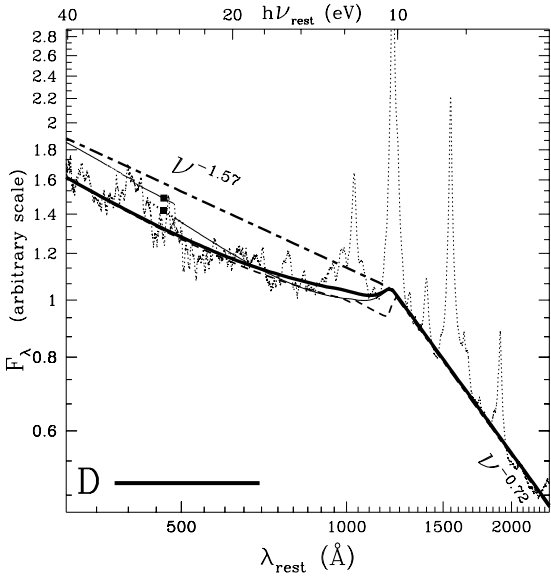


Fig. 5.— The dotted-line in this F_λ vs λ_{rest} plot represents the composite spectrum of radio-quiet quasars by TZ02. The straight short-long dashed line represents the intrinsic broken power-law SED assumed in Model D. It has a break at 1200 Å at which point the power-law index changes from -0.72 to -1.57 . The thick solid line overlaying the TZ02 data is Model D using the parameters listed in Table 1. As in Fig. 2, the thin continuous line represents the transmitted spectrum of an *individual* quasar with $z_Q = 1.0$ (using Model D parameters). The thin short-dashed line illustrates the discontinuity at $\lambda_{rest} = 1216$ Å if we set z_P to zero in Model D (i.e. without cavity).